Telemetry applications of SOQPSK and GMSK based modulation for airborne platforms

Conference Paper · December 2012

DOI: 10.1109/CODIS.2012.6422125

5 authors, including:

K. Krishna Naik
Indian Institute of Information Technology, Design and Manufacturing, Kurnool

Chinmoy Bhattacharya
Armament Research and Development Establishment (ARDE)

Telemetry Applications of SOQPSK and GMSK Based Modulation for Airborne Platforms

Umashankar Balasubramanian
National Flight Test Center(NFTC)
Aeronautical Development Agency(ADA)
Bangalore 560012, India.
Email: umashankar.ada@gmail.com

Pankaj R. Pacharne, Panga Radhakrishna,
K. Krishna Naik, C. Bhattacharya
Defence Institute of Advanced Technology
Girinagar, Pune 411025, India.
Email: cbhat0@diat.ac.in

***Abstract*—Bandwidth restrictions for flight test operations have led the designers world over to graduate from analog telemetry schemes to more compact digital telemetry schemes. Proper precoding and pulse shaping of non-return to zero (NRZ) waveforms are necessary prior to digital modulation for limiting the bandwidth of power spectrum of the NRZ pulses. The most common pulse shapes used are Gaussian filter for Gaussian minimum shift keying (GMSK), raised cosine filters, etc. Recently shaped offset quadrature phase shift keying (SOQPSK) is introduced as a bandwidth efficient modulation technique. In this paper, we report the bandwidth efficiency of SOQPSK for S-band airborne data links working at 4 Mbps rate [1]. Our results show that the SOQPSK-TG is the more bandwidth efficient modulation scheme than GMSK for telemetry applications.**

I. Introduction

Telemetry schemes currently functioning in most fighter aircrafts are analog (PCM/FM) schemes comprising of inputs from analog video and audio channels, data from analog vibration sensors, and digital PCM parameters from various other inputs. Quadrature phase shift keying (QPSK) and their offset version (OQPSK) are major varieties of digital modulation schemes those require less bandwidth compared to analog (PCM/FM) schemes. The abrupt phase changes between symbols in QPSK based schemes lead to envelope distortion with more power in the sidelobes of the spectrum [2].

The phase of the signal changes smoothly from one symbol to another symbol as a function of frequency pulse in continuous phase modulation (CPM). This ensures constant envelope modulation that reduces spectral re-growth and avoids signal distortion due to nonlinearity in high power amplifiers. The strength of the side lobe levels of the spectrum are further reduced by passing the modulating NRZ data through pre-modulation pulse shaping filters. Baseband pulse shaping smoothens the phase trajectory of signal, and hence stabilizes the instantaneous frequency over time.

The phase in CPM signal is [3]

$$\phi(t,\alpha) = 2\pi h \int_{-\infty}^{+\infty} \sum_{i=-\infty}^{+\infty} \alpha_i g(t - iT_s)dt. \quad (1)$$

Here, $g(t)$ is the frequency pulse, h is the modulation index. The phase of the signal is continuously varied with respect to $g(t)$. The coefficient α_i stands for the current pre-coded data bit depending on the modulation scheme of CPM. Gaussian minimum shift keying (GMSK) is a major variety of CPM where Gaussian frequency pulses are utilized for $g(t)$. Recently shaped offset quadrature phase shift keying (SOQPSK) is introduced as a bandwidth efficient modulation technique where data precoding and frequency pulse design take care for channels with higher premium on bandwidth.

In this paper, we discuss the design parameters of the frequency and phase pulses for GMSK and SOQPSK. Data pre-coding techniques for the CPM modulation schemes are shown through the Trellis diagrams depending on the changing input symbols. The actual trial results of PCM/FM, GMSK and SOQPSK in S-band transmission for flight telemetry applications at 4 Mbps rate are reported.

II. Analytical modelling of GMSK and SOQPSK modulation

A. GMSK Modulation Scheme

The phase function $\phi(t,\alpha)$ of GMSK modulation for $h = 0.5$ is

$$\phi(t,\alpha) = \sum_i (\alpha_i \frac{\pi}{2} \int_{-\infty}^{t-iT_s} g(t)dt). \quad (2)$$

Here, $\alpha_i = (-1)^i d_i d_{i-1}$ are the pre-coded output symbols and d_i is the i^{th} message bit to be transmitted. For GMSK, convolution of the gate function $rect(\frac{t}{T_s})$ with the Gaussian impulse response function $p(t)$ produces the frequency pulse $g(t)$where T_s is the symbol duration [4].

$$p(t) = \frac{1}{\sigma T_s \sqrt{2\pi}} \exp(-\frac{t^2}{2\sigma^2 T_s^2}) \quad (3)$$

The standard deviation $\sigma = \frac{\sqrt{ln(2)}}{2\pi BT_s}$ of $p(t)$ decides the 3-dB bandwidth of the GMSK modulated signal. As the BT_s product gradually increases to 1 the occupied bandwidth also increases leading to inter-channel interference. If BT_s decreases from 1 towards 0 the impulse response becomes wider that leads to inter-symbol interference and lesser bandwidth for modulated signal. The GMSK frequency pulse and its phase response are shown in Fig. 1. The frequency pulse in Fig. 1 is shown in continuous line, and the corresponding phase pulse is given in the dotted line. The smoothness of phase variation of modulated signal depends on the smoothness of the phase curve. The frequency pulse shown in Fig. 1 is for BT_s = 0.25 for telemetry applications, and the Gaussian pulse width is of two symbols duration. We have considered $\int_{-\infty}^{+\infty} g(t)dt$= 0.5 in this case. In the GMSK modulation scheme shown in Fig.

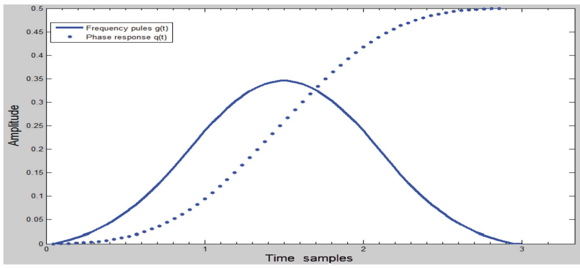

Fig. 1. GMSK frequency and phase pulses.

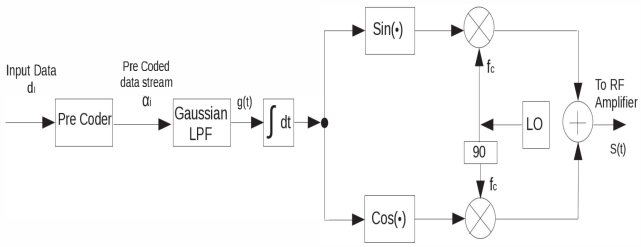

Fig. 2. GMSK modulation in I and Q channel representation.

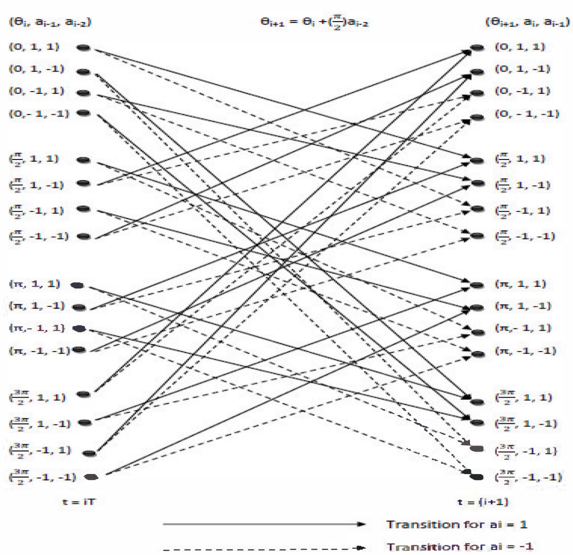

Fig. 3. Trellis diagram of GMSK.

2 the data stream is pre-coded prior to filtering with $g(t)$. The phase function $\phi(t, \alpha)$ is obtained by integrating the frequency pulse response. The phase modulated RF signal is produced by the in-phase and quadrature phase modulation shown in Fig. 2 that produces the GMSK output signal.

The phase and state variations of the pre-coded data in GMSK is shown in the Trellis state diagram of Fig. 3. This diagram shows the information of all possible output states with their possible phases. For each input state in the diagram there are two possible output states depending on the current message bit. The phase change of the current state depends on the previous phase and the previous message bit. In Fig. 3 the thick line represents the transition of state for bit 1 and the dotted lines represents the transition of state for bit 0. The four possible phases of output in GMSK for h=0.5 are 0, $\frac{\pi}{2}$, π, and $\frac{3\pi}{2}$ as shown in Fig. 3. Total 16 possible states occur depending on four possible phases and four possible combinations of message bits. This transition of states in the Trellis diagram is useful at the receiver to decode the transmitted symbols depending on the phase changes from one state to another.

B. SOQPSK Modulation Scheme

The modulation scheme with pre-coder and frequency pulse for SOQPSK is shown in Fig. 4. However, in SOQPSK the message bit stream is divided into in-phase (I) and quadrature phase (Q) channels, and one of them is delayed by half symbol time ($T_s/2$) duration as it happens for OQPSK. It is also called ternary CPM, as it generates $\alpha_i \epsilon \{-1, 0, 1\}$ from d_i using the precoding algorithm given in [5].

$$\alpha_i = \frac{(-1)^{i+1} d_{i-1}(d_i - d_{i-2})}{2}. \tag{4}$$

The ternary data α_i determines the phase transitions {-$\frac{\pi}{2}$, 0, +$\frac{\pi}{2}$} corresponding to α_i equals to {-1, 0, 1} such that α_i never assumes values {1,-1} for consecutive bits or vice versa. The

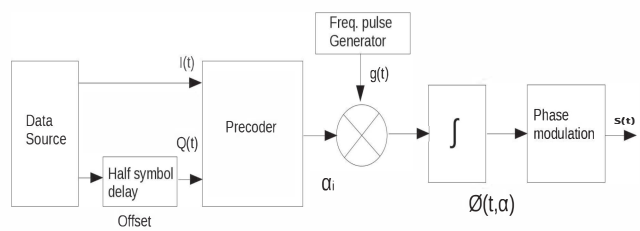

Fig. 4. Block Diagram of SOQPSK modulation scheme.

8 state transitions of precoder data for SOQPSK modulation is shown in the Trellis diagram of Fig. 5. Depending on the value of α_i two states are considered in the diagram, current state and the next state. Each state is represented in three bits with the MSB representing the status of the input whether it is I or Q. The MSB value of 1 stands for I channel data while Q channel data is represented with 0. The next bit and LSB together represent the present I-Q data at the precoder input. This I-Q symbol can take four possible values among {00, 10, 11, 01}, and are mapped to corresponding phase

states, e.g.,$\{\frac{\pi}{4}, \frac{3\pi}{4}, \frac{5\pi}{4}, \frac{7\pi}{4}\}$ respectively. Hence, each I-Q data corresponds to one phase state.

For example, consider the first state in Fig. 5 that is 000. In this case, the MSB represents the Q channel data present at precoder input having value either 1 or 0, with the present I-Q symbol as 00 specified by next bit and LSB together. Only one bit changes at a time as at the precoder input it is OQPSK. So here Q channel data would change while transiting to the next state with MSB. Hence, the next state would be either 100 or 101. Consider the next state is 101 with MSB as 1. Therefore, the terminating phase state is $\frac{7\pi}{4}$. Hence, the phase change occurred is -$\frac{\pi}{2}$. Assuming binary to antipodal mapping 0→1, 1→-1 so that the present I-Q symbol representing d_{i-2} and d_{i-1} have transition to -1 and 1 respectively. In this case the value of i is odd as we have considered the case for the Q channel. After substituting the values of data bits in (4) the value of α_i is -1, marked on the corresponding Trellis path.

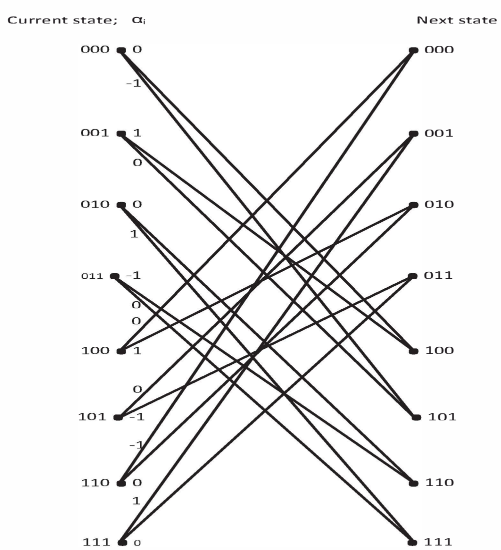

Fig. 5. State Trellis diagram for SOQPSK.

There are several varieties of SOQPSK scheme in which SOQPSK-TG is the most popular version as it achieves superior spectral containment of energy compared to other versions of SOQPSK. It can be viewed as hybrid of OQPSK and MSK. In MSK, $d_i \epsilon$ {-1, +1} whereas in SOQPSK-TG the precoded transition is between { 0, -1}, and {0, +1}. SOQPSK-TG frequency pulse is denoted by g_{TG}, and is expressed as [6]

$$g_{TG}(t) = n(t)w(t). \tag{5}$$

The raised cosine impulse response $n(t)$ is defined as [3]

$$n(t) = \frac{Acos((\pi \rho B t)/T_s)}{1 - 4(\rho B t/T_s)^2} \frac{sin(\pi B t/T_s)}{(\pi B t/T_s)} \tag{6}$$

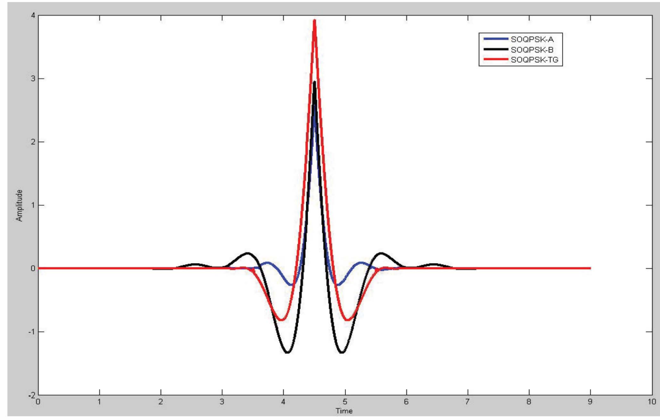

Fig. 6. SOQPSK frequency pulses.

and window function $w(t)$ is [3]

$$w(t) = \begin{cases} 1 & \text{for } |\frac{t}{T_s}| < t < T_1 \\ \frac{1}{2} + \frac{1}{2}cos\frac{\pi|\frac{t}{T_s}|-T_1}{T_2} & \text{for } T_1 < |\frac{t}{T}| < T_1 + T_2 \\ 0 & \text{for } T_1 < |\frac{t}{T}| < T_1 + T_2. \end{cases} \tag{7}$$

Where T_1 and T_2 together decides the time duration of frequency pulses after applying raised cosine window on it. The time domain plot of $g_{TG}(t)$ is shown in Fig. 6, and is compared with the other varieties such as SOQPSK-A and SOQPSK-B frequency pulses. The parameters for deriving these frequency pulses are given in Table I.

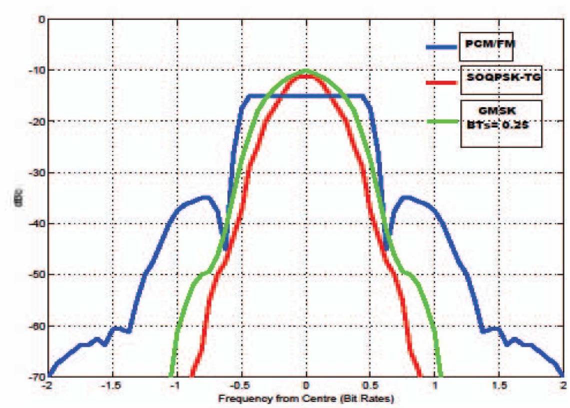

Fig. 7. Simulated Spectral Comparison.

TABLE I
FREQUENCY PULSE PARAMETERS.

Parameter	SOQPSK-A	SOQPSK-B	SOQPSK-TG
ρ	1.0	0.5	0.7
B	1.35	1.45	1.25
T_1	1.4	2.8	1.5
T_2	0.6	1.2	0.5

III. Results

The simulation results of spectrum plots of GMSK and SOQPSK-TG with respect to PCM-FM are shown in Fig. 7. We have utilized 4 Mbps data rate that is a comparable number for video, audio and other data streams required for digital telemetry [6]. It is seen from the spectrum plots that the SOQPSK-TG occupies the least of 99% bandwidth among the three modulation schemes, and the PCM-FM occupies the highest bandwidth. We now show the practical transmission results at S-band frequency of 2.3 GHz for a data rate of 4 Mbps in Fig. 8-10, and compare the bandwidth efficiency with the results of simulation shown in Fig. 7. The simulated 99% bandwidth of PCM/FM modulation in Fig. 7 is around 4.64 MHz that is $1.16R_b$, where R_b is the data rate. From the practical implementation in Fig. 8 the bandwidth occupied is 4.26 MHz. Similarly, for GMSK it is around 4.4 MHz in Fig. 7 that is $1.1R_b$, and the practical bandwidth occupancy in Fig. 9 is 3.6264 MHz. For SOQPSK-TG implementaion the 99% bandwidth is around 3.12 MHz in Fig. 7 that is $0.78R_b$ where as the practically occupied bandwidth in Fig. 10 is 3.11 MHz. This proves the efficiency of SOQPSK as the digital transmission scheme for S-band telemetry of airborne platforms.

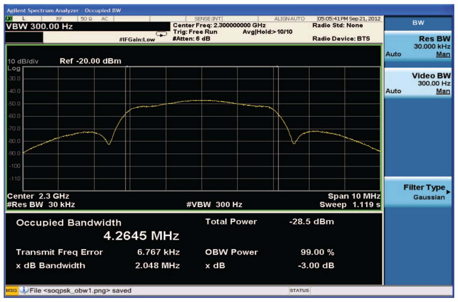

Fig. 8. Practical PCM-FM Spectrum at 4 Mbps in S-band.

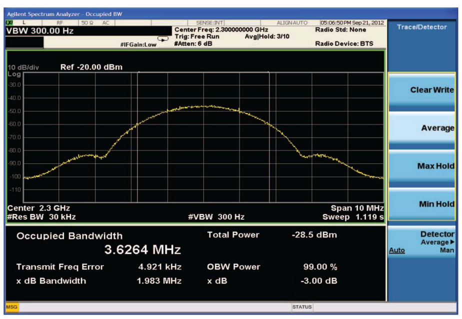

Fig. 9. Practical GMSK Spectrum at 4 Mbps in S-band.

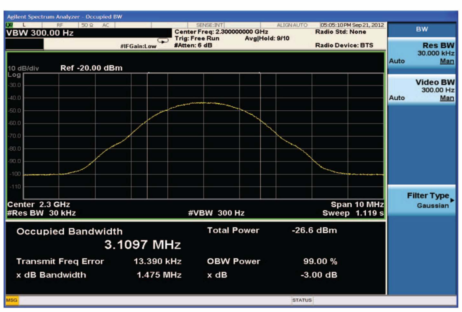

Fig. 10. Practical SOQPSK Spectrum at 4 Mbps in S-band.

TABLE II
Theoretical parameter values.

Characteristics	PCM/FM	GMSK	SOQPSK-TG
Link margin	3.73 Watts	2.34 Watts	3.73 Watts
99%bandwidth	4.64 MHz	4.4 MHz	3.12 MHz
Bandwidth efficiency	0.7	0.73	0.8

TABLE III
Practical result values.

Characteristics	PCM/FM	GMSK	SOQPSK-TG
99% bandwidth	4.26 MHz	3.63 MHz	3.11 MHz
Link margin	4.94 Watts	4.94 Watts	3.72 Watts

IV. Conclusion

We have reported here practical implementation along with theoretical simulations of power spectrum for SOQPSK-TG, GMSK modulation schemes compared to conventional analog PCM/FM telemetry schemes. Our results show that bandwidth efficiency of SOQPSK-TG scheme is a good choice for digital telemetry purposes. In arriving these results we have shown the detailed analysis of data precoding, and frequency pulses to be utilized for such transmission schemes.

V. Acknowledgement

Authors are thankful to the Director, ADA- Bangalore for granting project (Ref: ADA/NFTC/FTI/269) to DIAT, Pune.

References

[1] Umashankar Balasubramanian, V Remani, C Bhattacharya, "*Design of composite digital data frame for airborne platforms*", Proc. European Telemetry Conference, Munich, 12-14 June 2012.

[2] John G. Proakis *Digital Communications*, 4nd ed. Beijing: Publishing House of Electronics Industry, 2001.

[3] Terrance J. Hill, "*A non-proprietary, constant envelope, variant of shaped offset QPSK for improved spectral containment and detection efficiency*", MILCOM Conference Record, vol. 1, Los Angeles, California, pp. 347-352, October 23-26, 2000.

[4] CCSDS Standard 413.0-G-2,"*Bandwidth-efficient modulation*", Report Concerning Space Data System Standards, Space communication and Navigation Office, Space operations Mission Directorate, NASA Headquarters, Washington, DC, USA. 2009. (Available on-line at http://public.ccsds.org/publications/archive/413x0g2.pdf)

[5] IRIG Standard 106-04, "*Telemetry Standards*," Range Commanders Council Telemetry Group, Range Commanders Council, White Sands Missile Range, New Mexico, 2004. (Available on-line at http://www.ntia.doc.gov/osmhome/106.pdf.)

[6] Tom Nelson, Erik Perrins, and Michael Rice, "*Near optimal common detection techniques for shaped offset QPSK and Fehers QPSK*", IEEE Transaction on communications, Vol. 56, No. 5, May 2008.